Sauter, Caspar; Grether, Jean-Marie; Mathys, Nicole A.

Working Paper

A global compass for the great divergence: emissions vs. production centers of gravity 1820-2008

CESifo Working Paper, No. 7557

Provided in Cooperation with:
Ifo Institute – Leibniz Institute for Economic Research at the University of Munich

Suggested Citation: Sauter, Caspar; Grether, Jean-Marie; Mathys, Nicole A. (2019) : A global compass for the great divergence: emissions vs. production centers of gravity 1820-2008, CESifo Working Paper, No. 7557, Center for Economic Studies and ifo Institute (CESifo), Munich

This Version is available at:
https://hdl.handle.net/10419/198917

CESifo WORKING PAPERS

7557
2019

March 2019

A global compass for the great divergence: emissions vs. production centers of gravity 1820-2008

Caspar Sauter, Jean-Marie Grether, Nicole Andréa Mathys

CESifo

Impressum:

CESifo Working Papers
ISSN 2364-1428 (electronic version)
Publisher and distributor: Munich Society for the Promotion of Economic Research - CESifo GmbH
The international platform of Ludwigs-Maximilians University's Center for Economic Studies and the ifo Institute
Poschingerstr. 5, 81679 Munich, Germany
Telephone +49 (0)89 2180-2740, Telefax +49 (0)89 2180-17845, email office@cesifo.de
Editor: Clemens Fuest
www.cesifo-group.org/wp

An electronic version of the paper may be downloaded
· from the SSRN website: www.SSRN.com
· from the RePEc website: www.RePEc.org
· from the CESifo website: www.CESifo-group.org/wp

CESifo *Working Paper No. 7557*
Category 10: Energy and Climate Economics

A global compass for the great divergence: emissions vs. production centers of gravity 1820-2008

Abstract

We construct the world's centers of gravity for human population, GDP and CO_2 emissions by taking the best out of five recognized data sources covering the last two centuries. On the basis of a novel distorsion-free representation of these centers of gravity, we find a radical Western shift of GDP and CO_2 emissions centers in the 19th century, in sharp contrast with the stability of the demographic center of gravity. Both GDP and emissions trends are reversed in the first half of the 20th century, after World War I for CO_2 emissions, after World War II for GDP. Since then, both centers are moving eastward at an accelerating speed. These patterns are perfectly consistent with the lead of Western countries starting the industrial revolution, the gradual replacement of coal by oil and gas as alternative sources of energy, and the progressive catch up of Asian countries in the recent past.

JEL-Codes: Q560, Q590.

Keywords: center of gravity, growth, CO_2 emissions, GDP, population, great divergence.

Caspar Sauter
UBS Zurich / Switzerland
caspar.sauter@unine.ch

*Jean-Marie Grether**
University of Neuchâtel / Switzerland
jean-marie.grether@unine.ch

Nicole Andréa Mathys
Federal Office for Spatial Development
Bern / Switzerland
nicole.mathys@gmail.com

*corresponding author

September 2018
We thank Jim de Melo, Gabriel Felbermayr and Milad Zarin for insightful comments, as well as the Swiss National Science Foundation for financial support under grant 100018-136625. The usual caveats apply.

1. Introduction

The need for global indicators to address large-scale socio-economic issues is today more acute than ever. Human societies have become so opulent, ubiquitous and interconnected that many of the challenges they face, from climate change to security, find their roots and/or unravel consequences all around the planet. In spite of this globalization of economic problems, most measurement tools used by analysts and policy makers remain national in scope (e.g. Lindmark (2004)), or simply ag-gregated at the world level, without considering the geographical dimension except in specific cases (e.g. the indicators of remoteness (e.g. Baier and Bergstrand (2009)) or geopolitical importance (Reynaud and Vauday (2009)), but which are country-specific in nature). In this paper, we propose to revisit and refine the concept of the world center of gravity, which encapsulates into a single point the distribution of any variable upon the Earth's surface. We apply it to human population, gross domestic product (GDP) and anthropogenic carbon dioxide (CO_2) emissions, uncovering crucial but not trivial trends across the 1820-2008 period.

Early applications of the center of gravity (see Grether and Mathys (2010) and Quah (2011)) focused on GDP and recent decades. They unveiled a clear Eastern shift of the economic center of gravity since 1980. Two subsequent papers (Grether and Mathys (2011) and Grether et al. (2012)) extended the time period back in time, relying on the Maddison (2010) database. They identified a strong Western shift of the economic center of gravity during the 19th century, and a trend reversal towards the East in 1950. Although informative, these early studies are subject to three type of limitations: (i) the reported evidence so far is limited in its scope and its contribution to the under-standing of world challenges; (ii) the degree of accuracy depends on the availability and reliability of gridded data on the Earth's surface for the relevant variables and (iii) the center of gravity itself is a point beneath the Earth's surface, which is not entirely intuitive and leads to distorsions when its position is projected

upon a two-dimensional map. The objective of the present paper is to provide an appropriate treatment of each one of these caveats, thus illustrating the usefulness of the approach.

First, the inclusion of CO_2 emissions, along with GDP and population, allows for deeper insights into the period of the Great Divergence. Following Zhao et al. (2003), we use the demographic cen-ter of gravity as a benchmark, and construct simple measures of spatial imbalances to characterize the divergence between world GDP (or emissions) and world population. As could be expected, the two indices follow a similar inverted-u pattern over the centuries of the Great Divergence, but with two important differences: (i) the starting level of spatial imbalances for emissions is consider-ably larger than for production and (ii) the trend reversal occurs thirty years earlier for emissions (1920) than for GDP (1950). This illustrates the historic responsibility of the West, a cornerstone of the present negotiations to tackle Climate Change (e.g. Barrett and Stavins (2003) or Mattoo and Subramanian (2012)). It also proves how deeply associated are energy use and transition with the economic divergence or convergence processes (e.g. Bradshaw (2013)). Finally, it suggests that the industrial revolution was already full steam ahead when it began to materialize into significant shifts in economic power. This is in line with recent advances in economic history pointing to early roots of the process, perhaps as far back as the 16th century (e.g. Broadberry (2013) or Studer (2015)).

Second, an important limitation of all previous studies is that, for all years for which gridded data are not available, the assumption is simply that grid shares at the country level are kept unchanged with respect to the closest available year (e.g. 1990 for the papers based on the G-Econ database, see (Nordhaus et al., 2006)). This is of particular concern for countries like the US or China, which cover large areas, represent a significant share of world totals, and where the distribution of people and economic activity has suffered structural changes over the last two centuries. The present paper offers a welcome improvement with respect to that

shortcoming, by exploiting the Hyde 3.1 database (Klein Goldewijk et al., 2011), which provides gridded population data at a very disaggregated level. This database goes back as far as 1750, and has already been exploited by long run studies of land-use by human populations (Ellis et al., 2013) and its relationship with global warming (Matthews et al., 2014). This allows to spread national totals regarding GDP (or CO_2 emissions) according to varying population shares back in the past rather than by applying fixed shares.

Third, although the center of gravity ought to be seen as the tip of a global arrow originating from the center of the Earth, its representation on a two-dimensional map is subject to distorsions. The methodological section provides a thorough discussion of the distorsions affecting the two projection methods used so far (i.e. the orthogonal projection on the Earth's surface or onto a cylinder wrapping the Earth along the Equator). We then propose a new technique, which is distorsion-free, and consists of using two maps instead of a single one to represent the three Cartesian coordinates of the center of gravity. This allows to tracking with precision the evolution of the center of gravity.

In short, the center of gravity behaves like a global compass, with its length and direction depending on the spatial distribution of the corresponding variable upon the Earth's surface. Its calculation and comparisons across key socio-economic indicators allows unveiling global shifts and spatial unbalances over the sample period. This may justify further applications of the concept in a number of different domains, as suggested in the conclusion.

2. Methodology

2.1. Cartesian coordinates of world centers of gravity

Assume the surface of the Earth is covered by a regular grid of N cells. Each cell i, $i = 1, ..., N$, is identified by the latitude (ϕ) and longitude (λ) of its lower-left corner. For each cell, there is an estimate of the underlying variable V, i.e. CO_2 emissions (E) for the world emission center of gravity, GDP (G) for the world economic center of gravity, or population (P) for the world demographic center of gravity.

The Cartesian coordinates of each center of gravity are determined according to the three-step methodology previously introduced by Grether and Mathys (2010). First, the share of each cell in the world total is calculated, i.e. $s_{iV} = V_i \Big/ \sum_{i=1}^{N} V_i$. Second, the Polar coordinates of each grid cell are converted into their corresponding Cartesian coordinates, denoted by x, y and z. For that purpose, the Earth is assumed to be a perfect sphere, a reasonable assumption given the approximations affecting the measurement of the underlying variables. Cartesian coordinates may be expressed in kilometers, or as a fraction of the Earth's radius, R (6371km).[1] Third, the coordinates of the world center of gravity are obtained as weighted averages of the Cartesian coordinates of each grid cell, using grid cell shares as weights:

$$x_V = \sum_{i=1}^{N} s_{iV} x_i \ , \ y_V = \sum_{i=1}^{N} s_{iV} y_i \ , \ z_V = \sum_{i=1}^{N} s_{iV} z_i \qquad [1]$$

The obtained point, $P_V^* = (x_V, y_V, z_V)$, where $V = E, G, P$, locates within the sphere. The length of the associated vector, with its origin in the Earth's center, is obtained as:

[1] In a 3-dimensional space where the origin is at the center of the Earth, axis x (projection of the Greenwich meridian) and y (projection of the 90°E meridian) define the equatorial plane, and axis z is the North-South polar axis, the corresponding formulas are : $x_i = R\cos(\phi_i)\cos(\lambda_i)$, $y_i = R\cos(\phi_i)\sin(\lambda_i)$, $z_i = R\sin(\phi_i)$, where R is the Earth's radius. See the technical Appendix to Grether and Mathys (2011) for a detailed description.

$$\left\|\overrightarrow{OP_V^*}\right\| = \sqrt{(x_V)^2 + (y_V)^2 + (z_V)^2} \qquad [2]$$

This length can be used as a rough indicator of the concentration of the underlying variable on the Earth's surface. An extreme concentration in a single point would lead to a gravity center right on the Earth's surface, and a length just equal to the Earth's radius.[2]

2.2. Existing conventions to represent the location of world centers of gravity

The literature on how to map the Earth's surface on a two-dimensional plane dates back to more than two thousand years (see Snyder (1987) for a detailed survey including both technical and historical references). There is no universally accepted technique, as every method (cylindrical, conic or azimuthal, and their sub-cases) presents its shortcomings regarding specific distortions (e.g. on distances, areas or angles). The problem is further compounded here by the fact that the points we are interested in, i.e. the centers of gravity, are located within the sphere, not on its surface.

To the best of our knowledge, two projection techniques have been proposed till now for the world centers of gravity, as illustrated by Figure 1. The first one, proposed by Grether and Mathys (2010), consists of projecting orthogonally the center of gravity, P^*, upon the Earth's surface (Figure 1a). It leaves unspecified the technique used to represent the projection point, P_1, with latitude ϕ_1. The second technique, proposed by Quah (2011), directly projects the center of gravity on a cylinder wrapping the globe along the Equator (Figure 1b), which leads to a lower latitude for the projection point, $\phi_2 < \phi_1$.

[2] If the spatial distribution of the underlying variable is multimodal, a center of gravity close to the Earth's center does not necessarily imply less concentration. See Grether and Mathys (2011) for discussion.

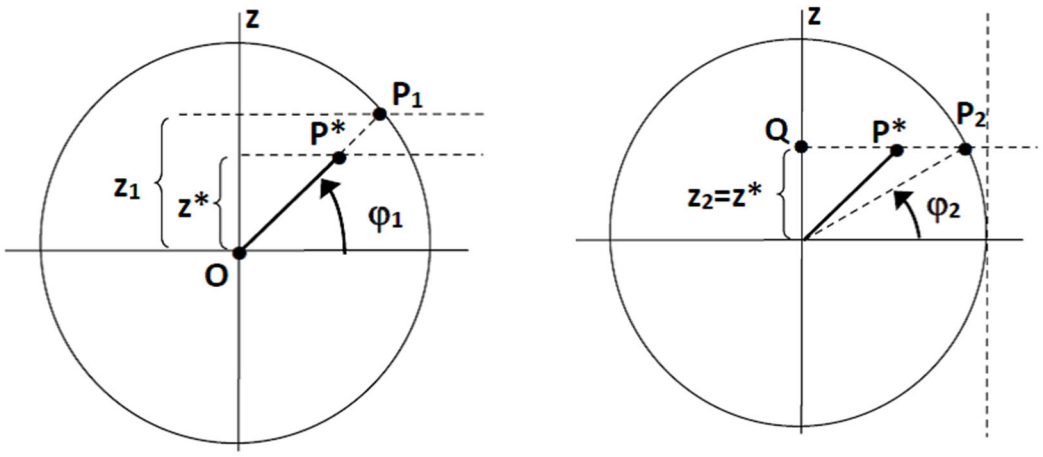

(a) Grether and Mathys (2010) (b) Quah (2011)

Figure 1: Alternative projections of the world's center of gravity

Both techniques may be criticized on the ground that they are insensitive to specific directional movements of the center of gravity, depending on the distribution of the underlying variable over time. The convention by Grether and Mathys (2011) does not capture changes of P^* along the OP_1 axis. The convention by Quah (2011) is insensitive to changes of P^* along the QP_2 line. Which type of changes matters more in practice is an empirical question, which could guide the choice between these two projection techniques, or any other alternative deemed more relevant depending on the specific variable or time period considered. However, any convention relying on a single two-dimensional map will remain affected by some kind of distortion. That is why we privilege here Cartesian over Geographic coordinates, and use two maps instead of a single one. We argue in the next subsection that this is the most accurate and tractable way to represent a point located deeply underground.

2.3. A new, distortion-free convention

The first map, on the left of Figure 2, is consistent with the technique of Quah (2011) that is, a cylindrical projection. It provides, on the vertical axis, a distortion-free representation of the z

Cartesian coordinate described in subsection 2.1. The horizontal axis represents longitude, which is subject to distortions, because there is an infinity of (*x, y*) combinations within the sphere corresponding to the same longitude. The second diagram on the right of Figure 2, provides an explicit representation of *x* and *y*, with the *x(y)* axis representing the projection of the Greenwich (90 degree) meridian. All three Cartesian coordinates are expressed as a fraction of the Earth's radius.[3]

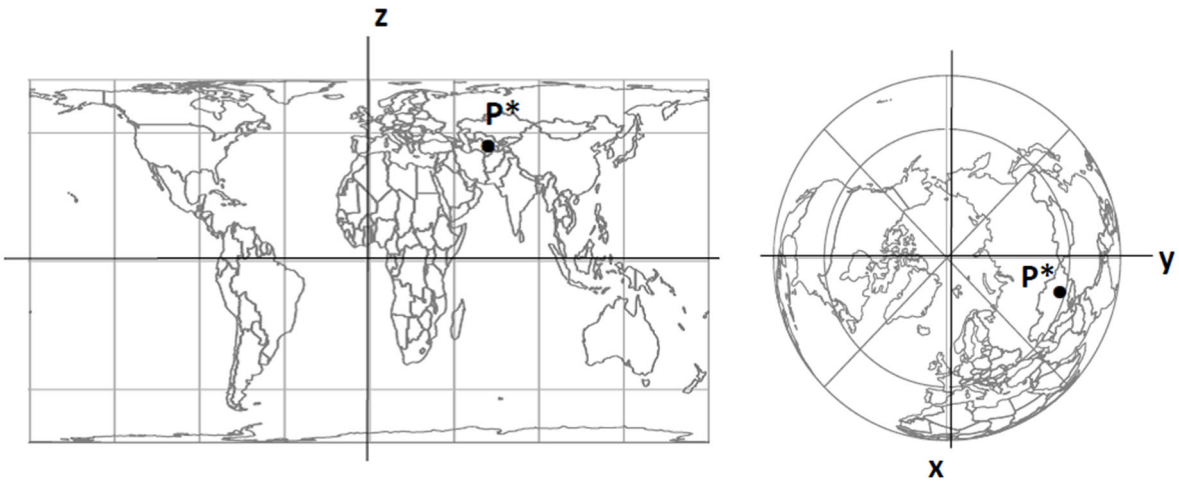

(a) cylindrical projection (b) azimuthal projection

Figure 2: Cartesian coordinates of the gravity center on two maps

The combination of these two maps allows describing without distortion any underground movement of the center of gravity, including those above-mentioned peculiar cases to which previously used conventions are insensitive. Two stylized examples will help to illustrate the complementarity of both maps. In each case, one of the two maps gives a confusing vision of the evolution of the center of gravity, while the other map unveils what actually happens. We

[3] Countries' contours correspond to a Lambert equal-area cylindrical projection in the left map, and to an azimuthal projection in the right map. Figures 2-4 limit the number of meridians and parallels to streamline presentation. Consecutive figures with actual results report meridians and parallels every 10°, along with ticks to indicate half of the Earth's radius on the *x,y,z* axis.

dub the first case the “wipper effect”. It is represented in Figure 3, where the left map suggests that the center of gravity shifts from point *A* to point *B*, then back again, and so forth, as a pendulum covering apparently the same horizontal distance period after period. However, what happens in reality, as shown by the right map, is that the center of gravity gets ever closer to the center of the Earth, along a zigzag trajectory analogous to the one of a bug crawling from the extremity of a car wiper to its rotating base. Again, this illusion is due to the fact that an infinity of within-sphere (*x, y*) combinations are compatible with the same longitude.

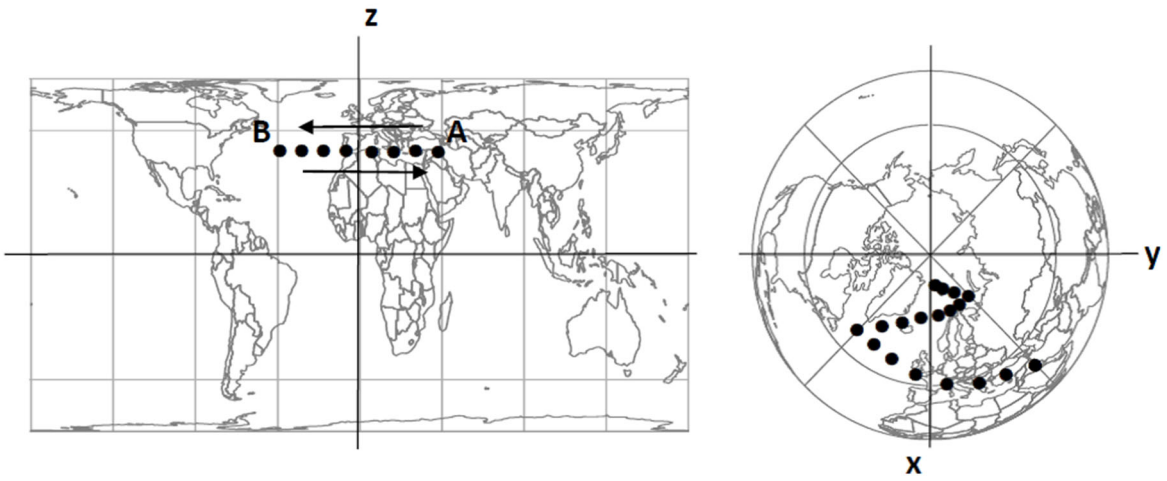

(a) (b)

Figure 3: The “wiper” effect

The right map is not exempt from optical illusion either. In the second case, illustrated in Figure 4, the center of gravity appears to be going round a regular ellipse on the right map. However, the left map shows that its height above the equatorial plane is regularly decreasing. We call that movement along a downward spiral a “staircase” effect.

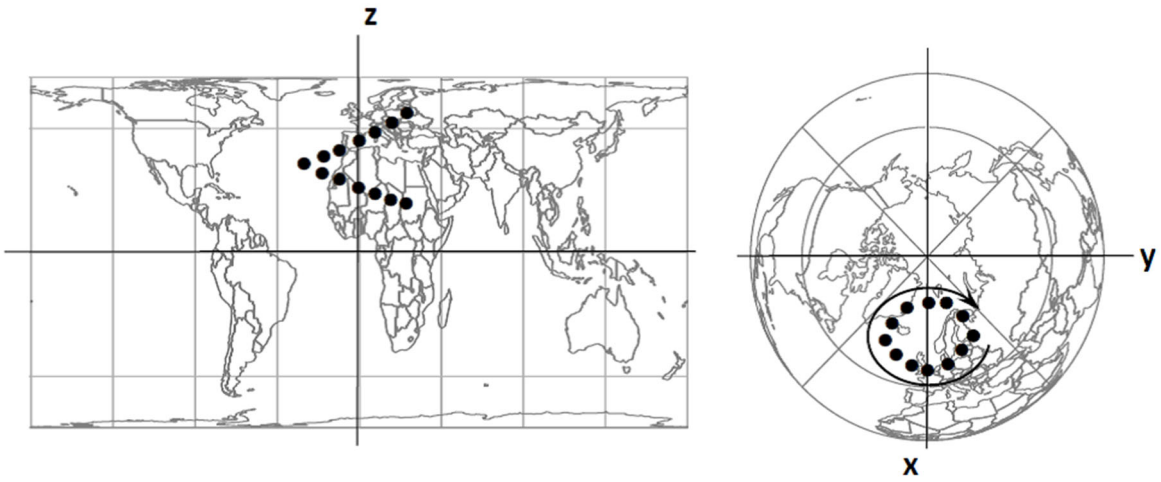

(a) (b)

Fig.4: the "staircase" effect

Other optical illusions could still be considered but are not reported here for the sake of conciseness, and as we limit the presentation to the two cases which do affect our own results. The key point is that, although we keep on using latitudes and longitudes to characterize locations on maps, the center of gravity is an underground point which is best identified in space by using three Cartesian coordinates rather than two Geographic coordinates.

3. Data sources

Data needed for calculations are obtained by combining five distinct data sources. On the one hand, three data bases provide information at the grid level. The HYDE 3.1 database (Klein Goldewijk et al., 2011) provides historical gridded population data from 10000 B.C to 2005 A.D. Since 1820, the data is available in 10 year intervals, and has a grid resolution of 5 by 5 arc minutes (one arc minute is equal to 1/60 of one degree). The G-Econ research project (see G-Econ (2011)) provides gridded GDP data at a one degree level of resolution for the years 1990, 1995, 2000 and 2005. The Emission Database for Global Atmospheric Research (EDGAR, see European Commission and Joint Research Centre/Netherlands Environmental Assessment Agency (2011)) reports yearly data on CO_2 emissions from fuel combustion and

non-metallic mineral processes (including cement production)[4], excluding short-cycle organic carbon from biomass burning at a 0.1° level of resolution. This data covers the period of 1970 to 2008. On the other hand, two other data bases cover larger periods but at the national level only, i.e. The Maddison Project (2013), which contains estimates of GDP and population from 1 to 2010 A.D., and the Carbon Dioxide Information Analysis Center (CDIAC, see Boden et al. (2013)), which provides CO_2 estimates from fossil-fuel consumption and cement production over the 1751-2010 period.

3.1. Population

The only modification of the HYDE database is to extend it from 2005 to 2010. To do so, we apply to each cell's population in 2005 the population growth rate 2005-2010 of the corresponding country as obtained from the national figures of the Maddison database. Country attribution of each cell is obtained by merging HYDE with the Global Database on Administrative Boundaries (GADM, 2012). As explained below, this HYDE gridded population database at a very high degree of resolution provides the basis to extend the GDP and emission gridded data backward in time.

3.2. GDP

First, the G-Econ 2005 gridded GDP data are extended to 2010, using Maddison country real GDP data for growth rates and by relying on the same method as described above for population. Second, we extend the gridded GDP series backward to 1820 in the following way. We combine the HYDE and the Maddison databases by assuming that within-country GDP is uniformly distributed per capita. This allows to spread national GDP figures from the

[4] Note that EDGAR covers more carbon dioxide sources, but to correctly match EDGAR with CDIAC (which covers only CO_2 emissions from fossil-fuel consumption and cement production), we retain from EDGAR only CO_2 emissions from IPCC source category 1A (fuel combustion) and 2A (non-metallic mineral processes).

Maddison database according to the gridded population shares obtained from the HYDE database. The obtained Maddison/HYDE gridded GDP figures are of course an approximation, but given data availability, it is the best way to capture within-country spatial variations backward in time. We then aggregate the so obtained 5 arc minutes cells to cells with a 60 arc minutes resolution in order to match them with the G-Econ data. Finally, we merge the Maddison/HYDE data, covering the decades 1820 to 2000, with the G-Econ database, which covers the years 1990 to 2010.[5] Whenever possible, we construct 5 year averages around decimal years to minimize the influence of potential extreme events.

3.3. CO_2 emissions

The procedure is similar to the one followed for GDP. First, gridded EDGAR emission data for 2008 are extended to 2012 by using 2008-2010 and 2010-2012 national growth rates obtained from the EDGAR FT2012 database (an extended version of EDGAR v4.2, containing country data). Second, to extend data backward in time, the HYDE and CDIAC databases are combined assuming emissions per capita are uniformly spread within countries. Then the obtained CDIAC/HYDE data are aggregated to a 60 arc minutes resolution to harmonize with the GDP aggregation level. Finally, we merge the CDIAC/HYDE data, covering the years 1820 to 1990 with the EDGAR database which covers the years 1970 to 2010.[6] Whenever possible, we construct 5 year averages around decimal years to minimize the influence of potential extreme events.

---

[5] To avoid potential jumps in the final series, we smooth the transition from one database to the other by using a mix of both cell GDP datasets for overlapping decades 1990 and 2000. For the year 1990, we calculate final cell GDP as 70% of Maddison/HYDE cell GDP and 30% of G-Econ cell GDP, while for the year 2000 we calculate it as 30% Maddison/HYDE cell GDP and 70% G-Econ cell GDP.

[6] To avoid potential jumps in the final series, we smooth the transition from one database to the other by using a mix of both cell CO_2 datasets for the years 1970, 1980 and 1990, as we did for GDP. For 1970 (1980, 1990), we calculate final cell CO_2 emissions as 75% (50%, 25%) of CDIAC/HYDE cell emissions and 25% (50%, 75%) of EDGAR cell emissions.

Table 1 and 2 display summary statistics for each variable after all described data treatments have been applied. Table 1 reports summary statistics for yearly series (1820 and 2010) that have been aggregated over all cells (thus corresponding to world real GDP, world CO_2 and world population). Table 2 reports summary statistics at the cell level for 1820 and 2010.

Table 1: Summary statistics (world level): Aggregated Population (persons), GDP (1990 USD), and CO_2 (gigagrams), 1820-2010

	1820	**2010**	**Annual growth rate 1820-2010 (%)**
Population	1.04E+09	7.23E+09	1.03
GDP	7.32E+11	6.49E+13	2.42
CO_2	15760	1.02E+07	3.60

Table 2: Summary statistics (cell level): Population (persons), GDP (1990 USD) and CO_2 (gigagrams), 1820-2010

Year	**Variable**	**Obs.**	**Mean**	**Std. Dev.**	**Min**	**Max**
1820	Cell Population	2120531	489.5	3643.4	0	772909
	Cell GDP	2120531	345335.5	1.58E+07	0	2.25E+10
	Cell CO_2	2120531	0.007	0.37	0	118.9
2010	Cell Population	2120531	3409.6	59676.9	0	5.84E+07
	Cell GDP	2120531	3.06E+07	1.35E+09	0	1.11E+12
	Cell CO_2	2120531	4.83	188.7	0	125099

4. Results

Figures 5, 6 and 7 report the two-map diagrams for the three centers of gravity, i.e. for population, GDP and CO_2 emissions. We remind the reader that the country frontiers are only reported here for graphical convenience. Normally the center of gravity itself always locates well below the Earth's surface. Its height (coordinates along orthogonal meridians) above (within) the equatorial plane is (are) given in the left (right) map.

Figure 8a compares the length of the gravity vectors, as the distance between the gravity center and the Earth's center. It is a rough measure of the concentration of the underlying variable on the Earth's surface. It also helps figuring out the radius of the inner-Earth imaginary concentric sphere upon which the center of gravity locates. Figure 8b compares the speed of the gravity centers, i.e. the distance they cover per decade.

Regarding interpretation of trends, the coordinates of the world center of gravity being a weighted average of individual cell's coordinates, it is intuitive that changes over time are mostly driven by variations in (large) country shares.[7] To condense presentation, we will only refer to the most important changes in the text below. The interested reader can also refer to the Appendix for the evolution of the share of the largest countries during the 1820-2010 period.

4.1. Population

As could be expected, the population center of gravity is basically located under Asia (Northern India in the left maps and along the Russian-Kazak frontier in the right maps). At the beginning of the period, its length is close to 5000 km, i.e. around $0.75R$, where R is the

[7] In theory, within-country variation should also be addressed, but in practice, most of the variation comes from between-country changes. See also Grether et al. (2012) for a more in-depth discussion of the underlying drivers and a decomposition of changes of the economic center of gravity into between-continent and within-continent effects.

Earth's radius (6371 km). This is the result of 0.5R elevation over the equatorial plane (corresponding to a Northern latitude of 30°) and approximately 0.6R rightward orientation on the projection of the 90° meridian (the coordinate along the projection of the Greenwich meridian is almost negligible). In short, human population is initially quite concentrated in the Asian part of the Northern hemisphere.

The bottom maps reveal a small but steady shift during the sample period, in two distinct phases. During the first phase, which lasts until 1910, the center of gravity shifts westward, with no latitudinal change. This is consistent with the gradual decline of China and India, whose combined share in world population drops from 55% to 40% along that sub-period. It is also concomitant with a leftward shift of the horizontal component of the left maps, and a corresponding decline in the length of the gravity vector by around 15%. That is, human population becomes more homogeneously spread, with a decline in Eastern and a rise in Western locations, in particular the USA.

During the second phase, starting in 1920, there is a clear Southern shift, slightly eastward until 1980, and westward since then. This is consistent with Western countries plateauing in terms of population, the combined share of China and India remaining roughly constant, and a relative increase of Southern countries in East Asia first, and in Africa second. Overall, there is again an increase in the dispersion of human population, although the decline of the length of the gravity vector is more moderate than in the first phase.

These shifts in the demographic gravity center are consistent with historical trends, but of mod-est magnitude, with an average speed of less than 200km per decade. The trends exhibited by the other two variables reveal more profound changes.

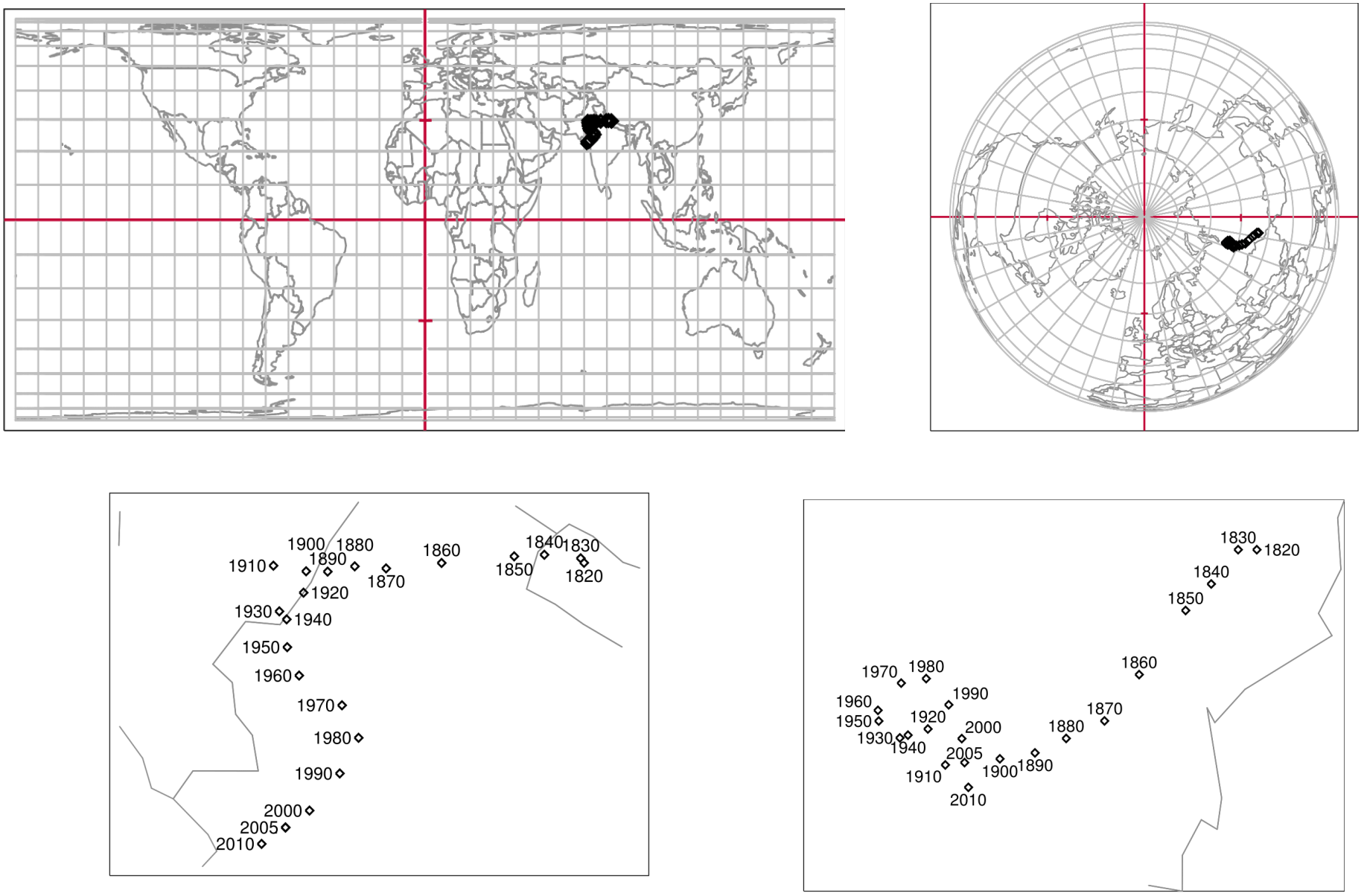

Figure 5: Center of gravity for population

4.2. GDP

The trajectory of the economic center of gravity is also in two phases, but the striking features are that apparent distances covered are far larger than for the demographic center, whereas the elevation upon the equatorial plane is almost unchanged, with most points locating along the 30◦N parallel on left-hand side maps. Starting 1820, the location is almost identical to the demographic center of gravity, reflecting the small differences in GDP per capita across countries prior to the industrial revolution. Then the Big Divergence leads to a strong western shift of the economic gravity center, with a speed two to three times larger than for the demographic center of gravity, and during a longer period. Although the 1930s and 1940s slow down the process, the immediate aftermaths of World War II brings it its last big western push, with a 1950 location close to the middle of the Atlantic. During that same sub-period, the combined share of China and India in world GDP has dropped from 45% to less than 10%, while that of the USA has risen from a few percentage points to more than 25%.

Since 1950, the eastward shift has been steady, driven by European reconstruction first, and then by the Asian comeback. It seems to accelerate a lot between 2000 and 2010, when the center of gravity jumps by more than 40◦ of longitude. However, while interpreting left maps, one has to remember that longitudes are not a precise concept in terms of distances. It does not only depend on latitude (which is here roughly constant), but also on the distance from the North-South axis, i.e. the inward location of the gravity center within the sphere, which is indicated on the right map. And, precisely between 2000 and 2010, it happens that the center of gravity gets quite close to the Earth center, ending a continuous decrease in the length of the vector since 1950. As a result, the effective speed in 2010 remains smaller than in 1950 that is, it is indeed large but not extraordinarily so. This explains the apparent jump and illustrates again how relying on a unique map to represent a three dimensional movement is misleading.

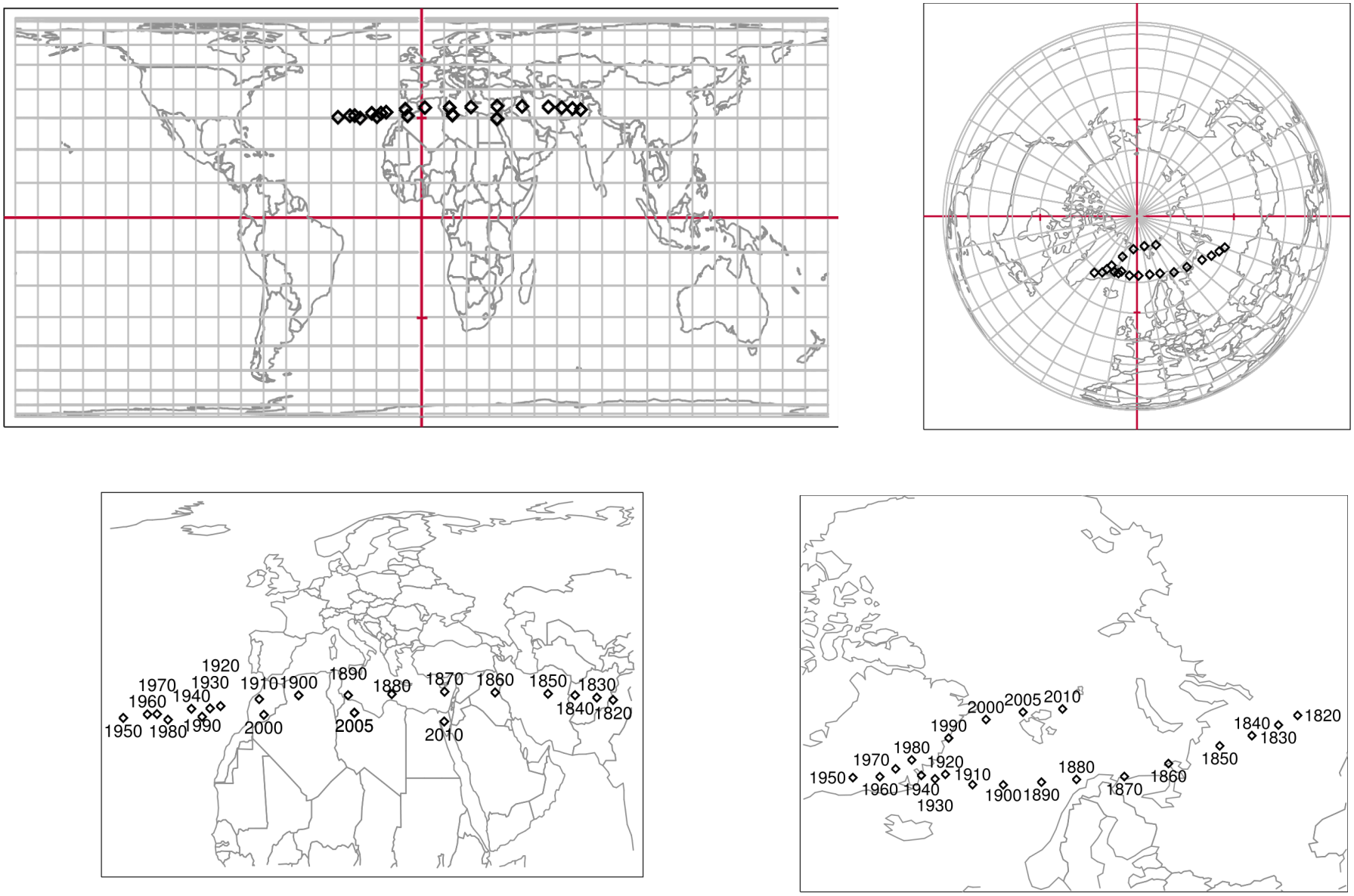

Figure 6: Center of gravity for GDP

4.3. CO_2 emissions

The trajectory of the center of gravity for emissions is even more remarkable than for GDP. It is initially an almost purely British phenomenon, with a center of gravity locating just underneath the UK, with a length corresponding to 98% of the Earth's ratio. As the industrial revolution spreads, and the use of coal as the main energy source with it, this center begins its descent towards the South-West and the Earth's center. Its most westward location is in 1920, when its projection gets close to the US coast and its length has decreased to 81% of the Earth's ratio. During that first period, the speed is similar to the one recorded for the economic center of gravity, although larger for the last two decades of the sub-period (1910 and 1920). Overall, the 19th century is a period during which GDP and CO_2 emissions tend to evolve synchronically and westward. This is due to the progressive replacement of the UK by the US as the major source of world emissions. US dominance peaks in 1920, with a share of 50% of world emissions.

Comparative dynamics of GDP and emissions are altered after World War I. While economic expansion pursues its westward trend, the center of gravity of CO_2 emissions shifts towards the East in 1930 and 1940. This suggests a decoupling between economic activity and pollution, which is probably linked with the early adoption of oil as an alternative, less emission-intensive, source of energy by the US (i.e. the major polluter), while other major polluters remain more coal-dependent. Indeed, according to Smil (2010), the share of coal in US energy supply peaks in 1910, while it does so only 40 years later in the UK and the USSR. As a result, the share of the US in world emissions declines strongly in 1930-1940, whereas its GDP share remains stable. This explains the earlier reversal of the emission center of gravity with respect to the economic one. Economic trends remain powerful however, and the US growth spurt following the end of World War II temporarily interrupts the eastern trend in

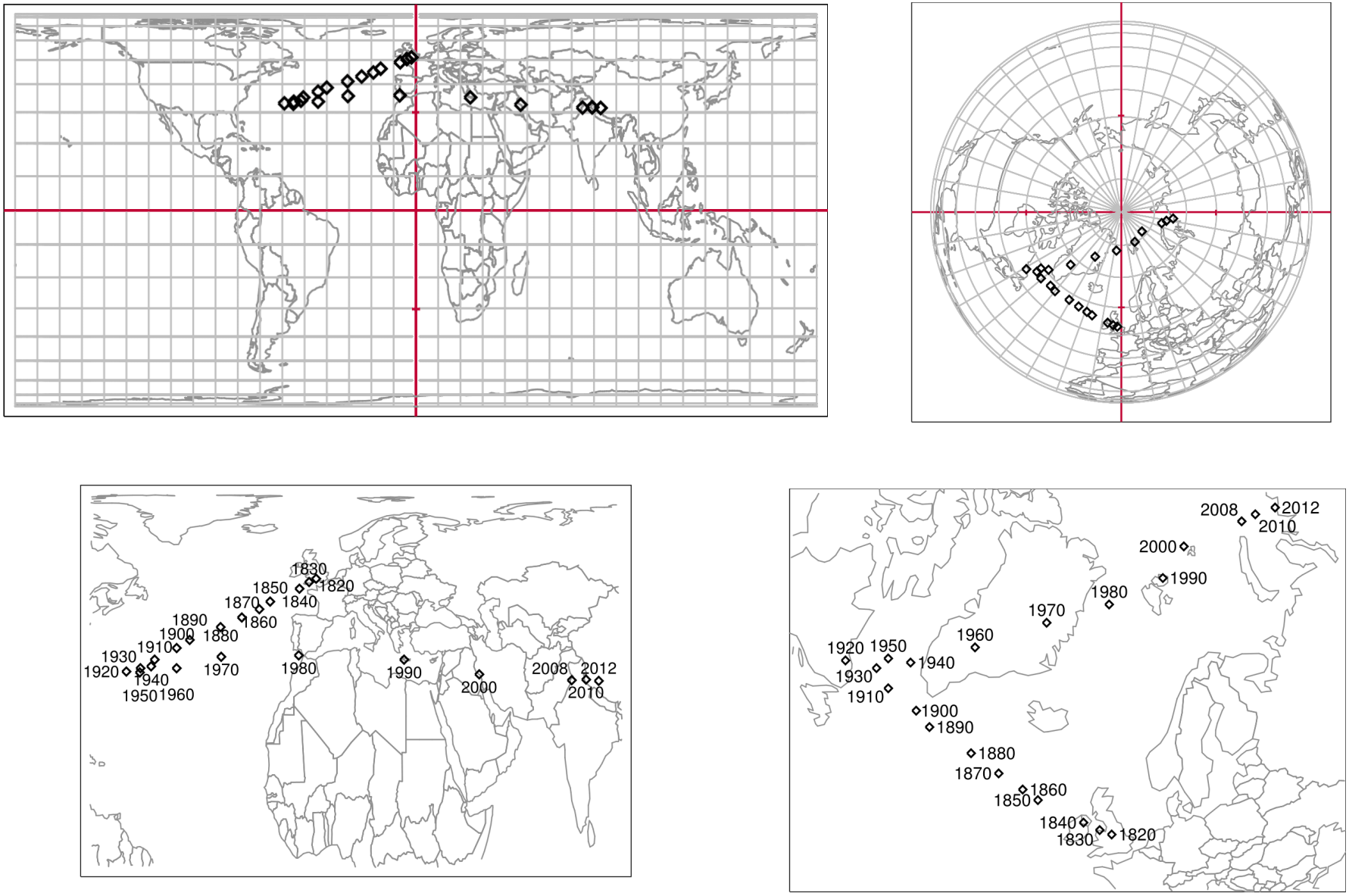

Figure 7: Center of gravity for CO_2 emissions

1950, when both centers of gravity shift westward again, albeit more modestly for the emission center.

From 1950 onward, the emission center of gravity is heading East, as the economic one. This is in line with a decline in US dominance in terms of both GDP and emissions, although the decline is a lot larger for emissions, with a US share in world emissions dropping from above 40% in 1950 to 20% in 1980. This coincides with very large distances covered by the emission center of gravity, close to 1000 km per decade, as reported by figure 8. This suggests again that the transition towards non-coal energy sources such as oil and gas has been quicker in the US compared to other large emitters (the share of coal falls below 50% as early as 1940 for the US, but only in 1960 for the UK or Japan, and 1970 for Russia, see Smil (2010).

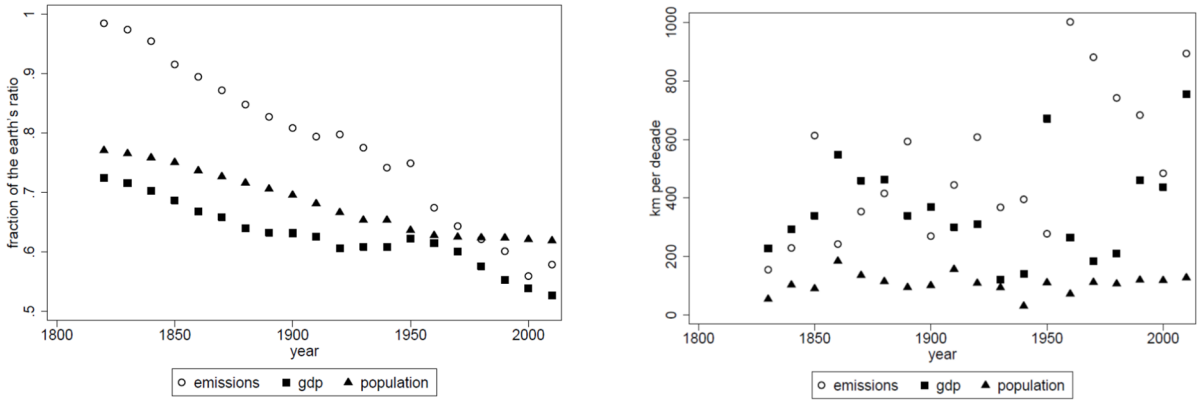

(a) length (b) speed

Figure 8: Length and speed for the centers of gravity

During the first two decades following the end of the cold war, 1990 and 2000, the eastern shift is slowed down, as the US share in world totals either stabilizes for emissions or even increases slightly for GDP. This is in line with a pause in the erosion of US dominance and the demise of the USSR.[8] But the movement accelerates again in the last decade, 2010, for

[8] We warn again the reader against using the left map only to estimate distances covered by the emission center of gravity in 1990 and 2000. They appear large, in particular in contrast

both GDP and emissions. This corresponds to the rise of Asian countries, in particular China, which remains heavily dependent on coal as an energy source. By the end of the sample period, the emission center of gravity locates quite close to the demographic center of gravity.

In a nutshell, the evolution of the emission center of gravity suggests radical changes in the spatial distribution of CO_2 emissions on the Earth's surface. In two centuries, it shifts from an extremely concentrated location to one which is strikingly similar to the distribution of world population. This calls for a complementary analysis in the last subsection.

5. Spatial imbalances: measurement and discussion

People are unequally spread across the planet's surface, i.e. mainly in the Northern Hemisphere, and mostly in Asia. This encapsulates into a location of the demographic center of gravity which is roughly stable over time, at $0.5R$ (R=6371km) above the equatorial plane and $0.5R$ to the right of the Greenwich meridian. If GDP and emissions were equally shared among people, the corresponding centers of gravity would locate at the same place, i.e. below Northern India, at roughly 70% from the center of the Earth. This is not what happened during the last two centuries. From there the idea of using the distance between the demographic center of gravity and the comparison one as a proxy for the spatial imbalances characterizing the per capita distribution of the underlying variable (either GDP or emissions).

More specifically, following Zhao et al. (2003), we define the index of spatial imbalances as the ratio between the actual distance between the demographic center of gravity and the one it is com-pared to, and the potential maximum for that distance, i.e. the length of the

with 1960. However, as shown by the right map, it is a typical "wiper" effect due to the fact that the center of gravity locates closer and closer to the Earth's center from 1950 onward. In reality distances covered are considerably smaller in 1990 or 2000 than in 1960 (see figure 8).

demographic center of gravity vector plus the Earth's radius.[9] Applied to GDP and emissions, this leads to the values reported in Figure 9.

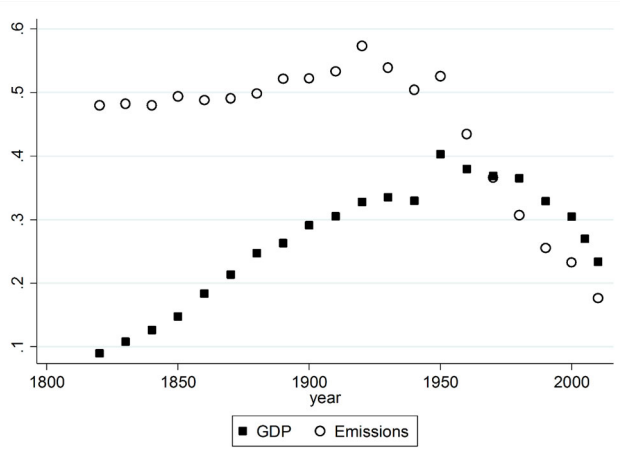

Figure 9: Indices of spatial imbalances

What happens for GDP confirms the trend reversal pattern already identified in figure 6. Spatial imbalances start below 10%, and then increase during the Big Divergence, as economic growth takes off in Western countries and their offshoots. The peak is reached in 1950, with an index slightly over 50%. After that, European and then most importantly Asian catch-up decrease spatial imbalances back to 20% at the end of the period.

The temporal pattern for emissions is distinct in that it starts from a large level of close to 50% in 1820. The rest of the trajectory is qualitatively similar to GDP, i.e. also an inverted-u shape, but with three differences. First, the rising phase is less steep, with a peak at 60%. This is due to the fact that, apart from going West, which increases the index, the center of gravity of emissions is also going down (Southward), which decreases the index. Second, as already

[9] For example, if the demographic center of gravity is denoted by *D*, the economic center of gravity by *G*, and the Earth's center by *O*, then the index of spatial imbalances for GDP is given by $\left\|\overrightarrow{DG}\right\| \Big/ \left[\left\|\overrightarrow{DO}\right\| + R\right]$, where R is the Earth's radius.

noticed in figure 7, the peak is reached in 1920, not 1950. Third, the decreasing phase is steeper, with a final index of spatial imbalances for emissions around 10% in 2010.

Intuitively, if data had been available for earlier centuries, it is quite probable that the pattern of spatial imbalances for emissions would have looked even more similar to the one for GDP. After all, before any country started its industrial revolution, differences in emissions per capita across countries were probably not large, implying a low level of spatial imbalances. This suggests a kind of leading role of emissions with respect to GDP over a long time span.

Although no formal analysis has been performed, the interpretation would be as follows. Start from a pre-industrial world where production and emissions are roughly homogeneous across people. Then technological innovation and the use of fossil fuels give an early boost to Western countries. The impact on emissions is immediate, while the effect on production takes several decades to materialize. During the rest of the 19th century and the early 20th century, as the West industrializes alone, emissions and production go hand in hand. Then the rapid adoption of less emission-intensive energy sources (oil and gas rather than coal) by the US sends back the emission center of gravity towards the East as early as the 1930s. Economic activity is characterized by more inertia, but when it starts to shift back as well after 1950, this accelerates further the eastern movement in emissions, also enhanced by the shift of more emission-intensive manufacturing activities towards Asia. As it happens, after a long period of divergence, both the economic and the emission centers of gravity seem to be dragged back to their initial 1820 location determined by demography.[10]

The above trends are confirmed when using alternative conventions regarding the smoothing shift from CDIAC to EDGAR data for emissions, or from Maddison to GEcon data for GDP.

[10] The extreme spatial concentration of emissions at the beginning of the sample period is due to the narrow definition of CDIAC historical data, limited to fossil fuel consumption and cement production only. However, to our knowledge, it is the best historical data on CO_2 emissions available at present.

Note that temporal patterns for the demographic and economic centers of gravity are similar to those identified by Grether et al. (2012), even though the latter did not rely on the Hyde database to capture within-country changes in spatial distributions. Moreover, as recently illustrated by Sauter et al. (2016), alternative hypothesis regarding the spatial distribution of emissions hardly affect overall patterns. Therefore, given data limitations, our results can be considered as reasonably robust.

6. Conclusions

Taking the best out of the available databases, this paper proposes for the first time distorsion-free representations of the trajectories of the world demographic, economic and emission centers of gravity over the last two centuries. Technological innovation, energy transition, structural change and wars are the main factors underlying the observed trends and turning points. In a nutshell, it is as if demography acts like a long run anchor, while emissions and GDP are two outcome variables of a technological diffusion process which increases spatial inequalities during the 19th century and progressively decreases them during the 20th century. The uncovered patterns allow for a quantification of the structural shifts underpinning the Great Divergence, but with a different time-frame depending on the underlying variable. When emissions are used instead of production, they suggest a deeper divergence, which starts well before 1820, and leads to an Eastern reversal as early as 1920. These results are in line with current research on the geopolitical origins of capitalism (e.g. Anievas and Nisancioglu (2015)). Based on these results, we suggest the following lines of further research.

Trade and FDI activities should be taken into account. For historical reasons first, as they were crucial in promoting the technological innovations at the root of the Industrial Revolution and the Great Divergence (e.g. O'Rourke et al. (2012)). For contemporaneous relevance also, as they are key elements of the globalization process, with a global diffusion

of the value chain that has made necessary the computation of trade in value-added flows (see OECD and WTO (2013)). Refining centers of gravity calculations in light of these increased interdependences may unveil interesting trends, for example to trace the potential consequences of the ”belt and road” policy recently adopted by China (The Economist (2017)), or to capture consumption-based rather than production-based CO_2 emission estimates (e.g. Wiebe and Yamano (2015)), a distinction that is at the heart of climate change negotiations today.

Moreover, further research should aim at including even more variables, to capture the many dimensions of human activities and interdependences. To mention just one case, in a world that has become more multipolar, large nations rely increasingly on geopolitical power (energy, geography, nuclear and military force) or soft power instruments (trade again, but also diplomacy, advertising, or cultural promotion) to improve their relative positions (e.g. Reynaud and Vauday (2009) or Wang et al. (2015)). This may lead to a frequent rebalancing of socio-economic influences at the world-wide level. By synthesizing the spatial distribution of any variable into a single point, the world center of gravity approach allows to reveal interesting dynamics within this changing context.

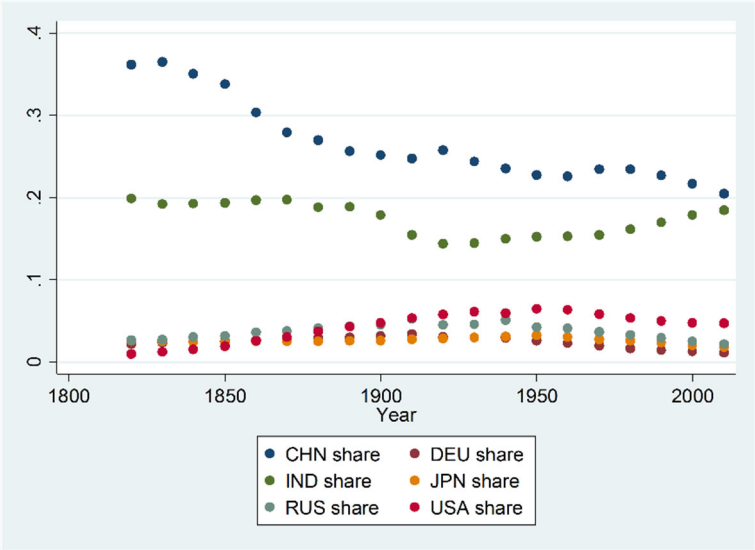

(a) Population

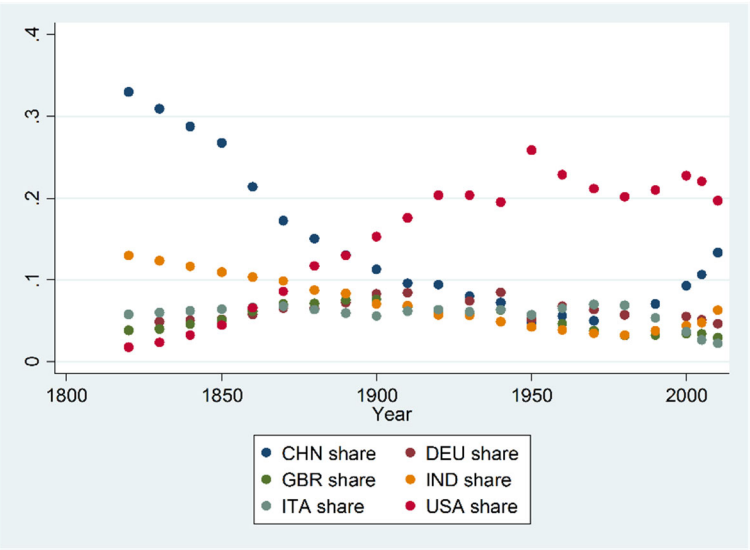

(b) GDP

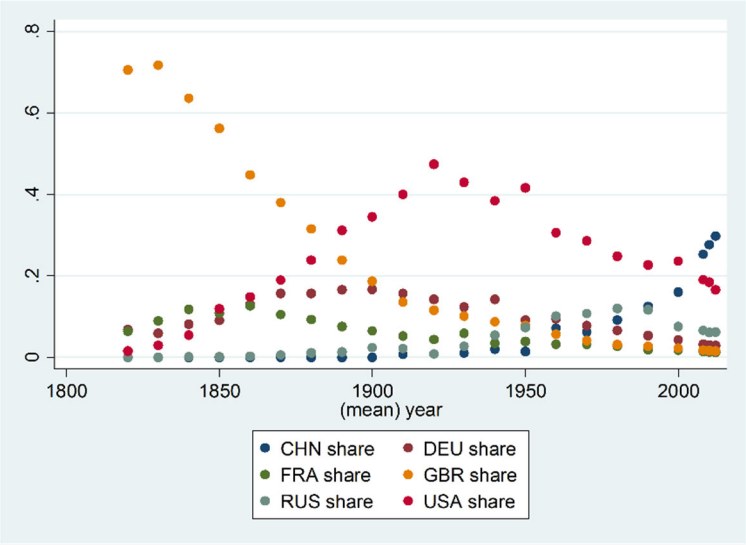

(c) Emissions

Figure A1: Shares of major countries in world totals 1820-2010

References

Anievas, A. & Nisancioglu, K. (2015). *How the West Came to Rule - The Geopolitical Origins of Capitalism*. University of Chicago Press.

Baier, S. L. & Bergstrand, J. H. (2009). Bonus vetus ols: A simple method for approximating international trade-cost effects using the gravity equation. *Journal of International Economics* 77 (1), 77 – 85.

Barrett, S. & Stavins, R. (2003). Increasing Participation and Compliance in International Climate Change Agreements. *International Environmental Agreements: Politics, Law and Economics* 3 (4), 349–376.

Boden, T., Marland, G., Andres, R. (2013). Global, regional and national fossil-fuel CO_2 emissions. Tech. rep., Carbon Dioxide Information Analysis Center, Oak Ridge National Laboratory, U.S. Department of Energy, Oak Ridge, Tenn. USA.

Broadberry, S. (2013). Accounting for the great divergence. Economic history working paper no 184-2013, London School of Economics.

Ellis, E. C., Kaplan, J. O., Fuller, D. Q., Vavrus, S., Goldewijk, K. K. & Verburg, P. H. (2013). Used planet: A global history. *Proceedings of the National Academy of Sciences* 110 (20), 7978–7985.

European Commission, Joint Research Centre (JRC)/Netherlands Environmental Assessment Agency (PBL) (2011). Emission database for global atmospheric research (EDGAR), release version 4.2. URL http://edgar.jrc.ec.europa.eu

G-Econ (2011). Geographically based economic data. URL http://gecon.yale.edu

GADM (2012). GADM database of global administrative areas, version 2.0. URL www.gadm.org

Grether, J.-M. & Mathys, N. A. (2010). Is the world's economic centre of gravity already in Asia? *Area* 42 (1), 47–50.

Grether, J.-M. & Mathys, N. A. (2011). On the track of the world's economic center of gravity. In: de La Grandville, O. (Ed.), *Frontiers of Economics and Globalization*, Vol.11: Economic Growth and Development. Emerald Group, London, pp. 261–287.

Grether, J.-M., Mathys, N. A. & Lutzelschwab, C. (2012). L'essor et le déclin de l'occident: une perspective géographique. *Revue d'économie du développement* 2, 31–56. URL English version available at:http://works.bepress.com/nicole_mathys/11/

Klein Goldewijk, K., Beusen, A., van Drecht, G. & de Vos, M. (2011). The Hyde 3.1 spatially explicit database of human-induced global land-use change over the past 12,000 years. *Global Ecology and Biogeography* 20 (1), 73–86.

Lindmark, M. (2004). Patterns of historical CO_2 intensity transitions among high and low-income countries. *Explorations in Economic History* 41 (4), 426 – 447.

Maddison, A. (2010). Statistics on world population, GDP and per capita GDP. URL http://ggdc.net/MADDISON/

Matthews, H. D., Graham, T. L., Keverian, S., Lamontagne, C., Seto, D. & Smith, T. J. (2014). National contributions to observed global warming. *Environmental Research Letters* 9 (1), 014010.

Mattoo, A. & Subramanian, A. (2012). Equity in Climate Change: An Analytical Review. *World Development* 40 (6), 1083–1097.

Nordhaus, W., Azam, Q., Corderi, D., Hood, K., Makarova, N., Mohammed, M., Miltner, A. & Weiss, J. (2006). The G-Econ database on gridded output: methods and data. URL http://gecon.yale.edu

OECD, WTO (2013). Measuring trade in value added: An OECD-WTO joint initiative. URL http://www.oecd.org/sti/ind/measuringtradeinvalue-addedanoecd-wtojointinitiative. htm

O'Rourke, K. H., Rahman, A. S., & Taylor, A. M. (2012). Trade, Technology and the Great Divergence. Departmental Working Papers 35, United States Naval Academy Department of Economics. URL https://ideas.repec.org/p/usn/usnawp/35.html

Quah, D. (2011). The global economy's shifting center of gravity. *Global Policy* 2 (1), 3–9.

Reynaud, J. & Vauday, J. (2009). Geopolitics and international organizations: An empirical study on IMF facilities. *Journal of Development Economics* 89 (1), 139 – 162.

Sauter, C., Grether, J.-M. & Mathys, N.A. (2016). Geographical spread of global emissions: Within- country inequalities are large and increasing. *Energy Policy* 89 (C), 138–149.

Smil, V. (2010). *Energy Transition: History, Requirements, Prospects*. Praeger, Santa Barbara, CA.

Snyder, J. (1987). Map Projections: A Working Manual. No. 1395 in US Geological Survey Professional Paper. US Government Printing Office, Washington.

Studer, R. (2015). *The Great Divergence Reconsidered: Europe, India, and the Rise to Global Economic Power*. Cambridge University Press.

The Economist (2017). The new silk route: All aboard the belt-and-road express. May 4th.

The Maddison Project (2013). 2013 version. URL http://www.ggdc.net/maddison/maddison-project/home.htm

Wang, S., Cao, Y. & Ge, Y. (2015). Spatio-temporal changes and their reasons to the geopolitical influence of China and the US in South Asia. *Sustainability* 7 (1), 1064-1080.